Proceedings of Global Power and Propulsion Society
ISSN-Nr: 2504-4400
GPPS Xi'an21
18th – 20th October, 2021
www.gpps.global

GPPS-TC-2021-0034

AERODYNAMIC AND STRENGTH IMPROVEMENT OF THE AXIAL TURBINE OF A HELICOPTER GTE

G.M. Popov
Samara National Research University
grishatty@gmail.com
Samara, Russia

Evgenii S. Goriachkin
Samara National Research University
goriachkin.e.s@gmail.com
Samara, Russia

Oleg V. Baturin
Samara National Research University
oleg.v.baturin@gmail.com
Samara, Russia

A.I. Korneeva
Samara National Research University
akorneeva94@mail.ru
Samara, Russia

Igor Egorov
Moscow Aviation Institute National Research University
egorov300657@yandex.ru
Moscow, Russia

ABSTRACT

The paper presents the results of solving the complex problem of improving strength and efficiency of a single-stage axial turbine of a small-sized helicopter GTE using multidisciplinary optimization methods. An analysis of the initial turbine showed that the strength reserve of the working blade was significantly lower than that required by the strength standards. In order to eliminate the problem at the first stage the task of rotor wheel adjustment only according to strength requirements without taking into account aerodynamic processes was solved. As a result, the turbine rotor wheel variants that met the strength limitations were obtained. These results were the starting point for aerodynamic optimization. The optimisation has resulted in a compressor turbine variant that meets the strength standards with an efficiency close to the initial compressor turbine variant.

INTRODUCTION

The article describes research into the design of an axial uncooled compressor turbine (hereinafter in the text the abbreviation CT is used) (Figure 1) of a promising small turboshaft engine using multidisciplinary aerodynamic and structural optimization. The turbine under study was an axial and uncooled. This turbine is designed to rotate the compressor of the helicopter engine. The engine also has a second turbine to rotate the propeller. The turbine in question is a new development and there is no published material on the previous stages of its construction.

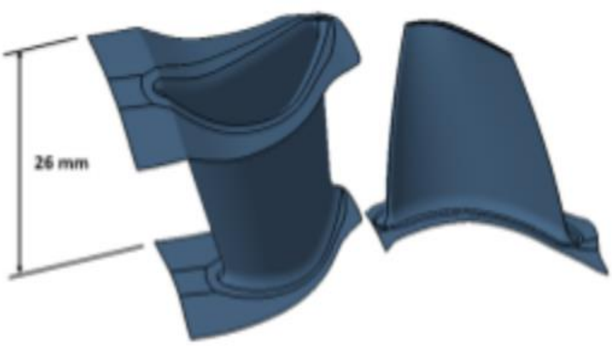

Figure 1 The turbine under investigation

During the refinement of the engine design, it became necessary to significantly increase the gas temperature at the combustion chamber outlet. After that, the strength margins of the turbines became significantly lower than the requirements to the strength margins of gas turbine engines by the standards and regulations existing in the Russian

Federation for civil aviation aircraft. It was found that the local long term strength factor of the RW CT is 52 % less and than required by the strength standards. The long-term load-bearing capacity factor of RW CT is 39 % less than that required by the strength standards. Thus, in order to obtain an acceptable turbine design, the shape of the blades must be modified to ensure that the reliability requirements are met. The maximum possible efficiency of the turbine should be achieved.

To solve this problem, it was decided to use aerodynamic and strength optimization methods with 3D numerical working process models and 3D strength models of working blades.

PROBLEM SOLVING ALGORITHM

The optimization algorithm used for simulation the turbine is shown in the block diagram in the Figure 2. The optimization process is an iterative process. Before it is started a variant of the turbine flow path configuration is formed and its parameters are calculated (either strength only or aerodynamic and strength only). In the first step, the IOSO optimizer program generates a vector of variable parameters x_1, x_2, x_3, …, x_n. This vector represents the values of the variables of the parametric blade model created in the Numeca AutoBlade program. On the basis of these values, files with 3D geometry of the blade airfoil are generated, which are automatically loaded into the grid generator program Numeca AutoGrid, where a grid model of the turbine flow path is created. The mesh generator program and special macros are also used to export the geometry of the RW blades to the Ansys APDL strength analysis program. Then 3D CFD modelling of the working process and calculation of RW strength parameters in 3D is performed. Moreover, CFD calculations and strength modelling can be done together, or a calculation can be disabled if it is not required. As a calculation result, a vector of output parameters y_1, y_2, y_3, … y_n is formed, which represents the values of working process parameters and/or strength for the formed turbine version. On the basis of the output parameters vector using optimization algorithms, the IOSO program creates a new combination of initial data (turbine configuration) and the solution of the task continues until the required result is achieved.

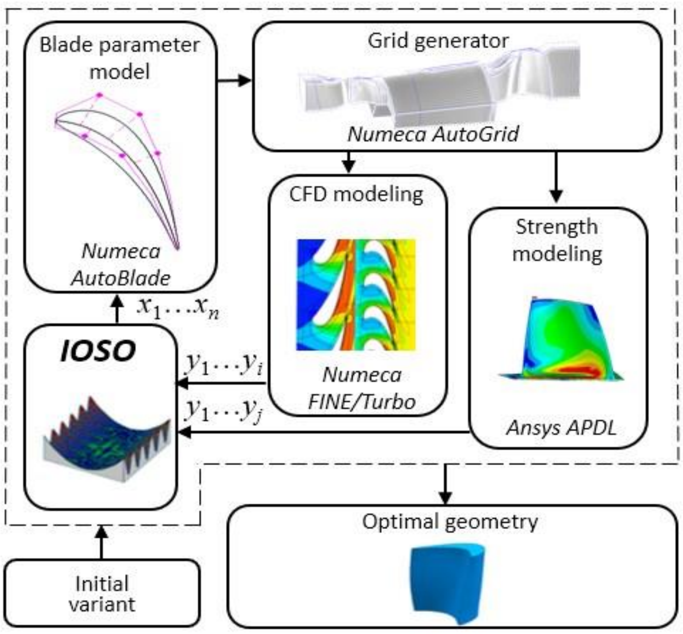

Figure 2 Process chain used in the research.

Operation of the process chain implemented in the IOSO program is based on the technology of building a response surface [1, 2]. To create an initial search area, IOSO uses a random number generator within a given range of variable values (initial search area). The initial variant of CT was set as the original variant in the optimization process.

CREATION AND VERIFICATION OF THE CFD TURBINE MODEL

Numerical model of the turbine working process was created on the basis of geometric models of the original CT in the Numeca FINE/Turbo software package (Figure 3). The following assumptions were made when creating the calculation models. Modeling was performed in 3D stationary axisymmetric formulation. Thermal deformations of the flow path and deformation of the RW from the action of centrifugal force were taken into account.

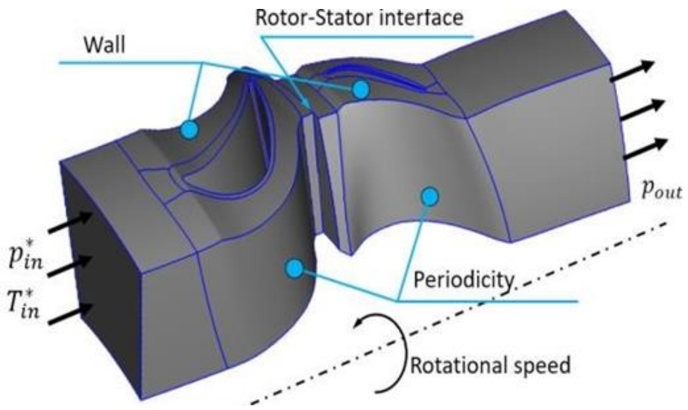

Figure 3 Numerical model of a compressor turbine working process with boundary condition

Radial diagrams of total pressure and total temperature distribution were given as boundary conditions at the turbine inlet. The direction of flow angle at the turbine inlet was assumed to be axial. Static pressure at the turbine outlet was set at the hub radius. The pressures at the other radiuses were calculated according to the radial equilibrium equation. The static pressure at the turbine outlet was set according to the required degree of expansion.

A Full Non Matching Mixing Plane type interface built into the software system was used to transfer data between the areas of the NB and RW.

The Spalart-Allmaras model was used as a turbulence model.

As no experimental data are available for the planned turbine, grid studies were performed to select the grid model settings using the methodology developed by the authors on the other turbines [3, 4].

Three parameters were chosen to characterize the computational grid settings. The number of cells per mesh layer was defined by the B2B parameter, which was calculated as the ratio of the total number of elements in the mesh to the number of mesh layers. The number and distribution of cells by height of the flow path was characterized by the following parameters (Figure 4):

ER is the cell growth factor in the near-wall area. Shows how many times the height of the next cell y_i is less than the previous cell y_{i-1};

MR - maximum height of the cell in the channel. Defined by the ratio of the maximum cell height in the channel y_{max} to the size of the cell closest to the wall y_{min}.

In total, 10 mesh models were created with different settings. The parameters characterizing the mesh models are shown in Table 1, with the total number of cells in the mesh in brackets.

Table 1 CT grid settings for perfoming grid studies

B2B (thousand in one layer / million total)	-2 (16.3/1.4)	-1 (29.6/2.1)	0 (44.5/2.9)	1 (69.5/4.1)
ER, (mln)	1.2 (1.5)	1.4 (1.2)	1.6 (1.0)	1.8 (0.96)
MR, (mln)	250 (1.4)	500 (1.2)	1000 (1.06)	2000 (0.93)

In all grid models, a value $y_+ = 1$ has been ensured.

A series of calculations were carried out during the grid studies where one parameter was varied in the base grid with parameters B2B0, ER=1.4 and MR=500, while the other two parameters remained unchanged.

An analysis of the grid model parameters' influence on the values of integral parameters of the turbine and the height distribution of the parameters was carried out. The analysis showed that a change in the B2B parameter has almost no effect on the radial distribution of the parameters, but has an effect on their integral values. In contrast, the ER and MR parameters have an effect on the radial distribution of the turbine parameters, but have almost no effect on the integral values.

The influence of the B2B parameter on the integral parameter values was estimated by plotting the dependence of the B2B parameter on the ratios of the calculated flow rate, efficiency and compression ratio to the values of the same parameters calculated on the heaviest B2B1 grid (Figure 4 a).

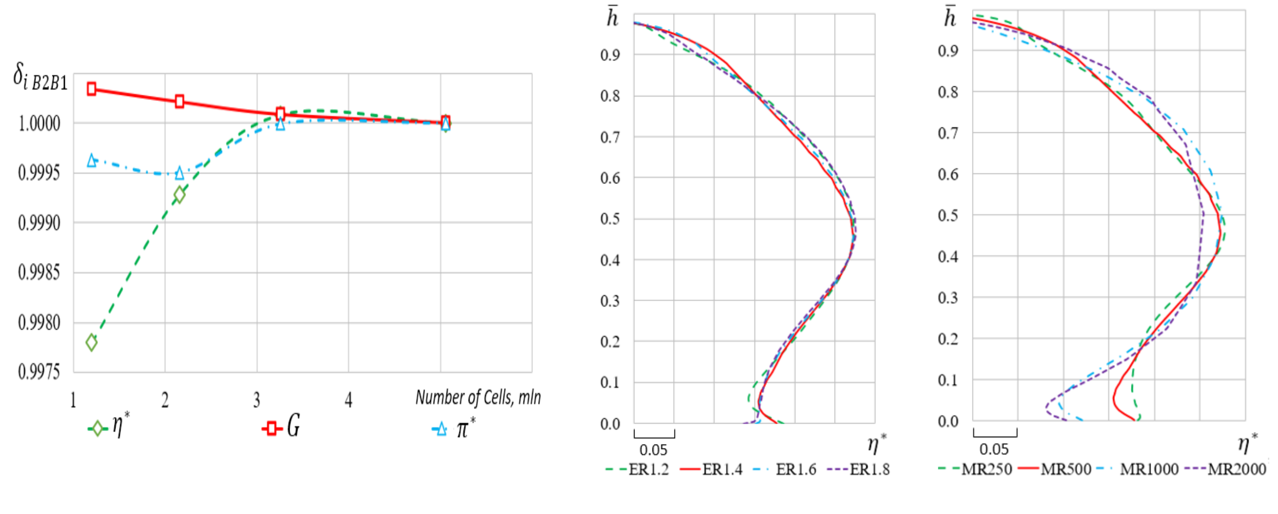

Figure 4 Influence of the selected parameters on the working process modelling of the investigated turbine: a - B2B; b - ER; c - MR

Figure 4 shows that the parameter values calculated on grid B2B0 are almost identical to those calculated on grid B2B1 meaning that there is grid convergence on the B2B0 grid. However, the parameter values calculated on the lightest grid B2B-2 and the heaviest grid B2B1 are not significantly different in absolute values. Thus, in order to save of optimization, grid B2B-2 was used and the most detailed grid B2B1 was used to verify the results.

A comparison of the calculated parameter distributions over the height of the CT at different values of ER and MR (Figure 4 b, c) shows that using ER parameter more than 1.4 leads to flow structure change in the area of 0 to 0.1 of relative flow path height, and using MR parameter more than 500 leads to flow structure change in the area of flow core, as well as in relative height of 0 to 0.2 of relative flow path height. Therefore, it was decided to use a grid with ER=1.4 and MR=500 parameter values, as it has fewer elements, and for checking the results the most detailed grid with ER=1.2 and MR=250 was used.

MODEL FOR STRENGTH CALCULATION

The strength model of RW CT was implemented in Ansys Mechanical APDL. The algorithm for automated construction of the strength model of the CT working blade is shown in Figure 5.

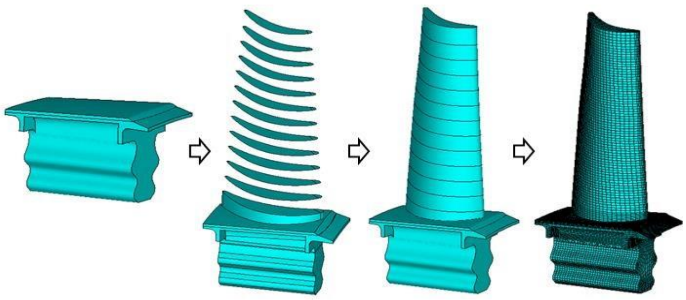

Figure 5 A process for creating a strength model of CT working blade

The temperature distribution over the CT blades was set as initial data in the form of a temperature distribution over the blade height. The temperature in the blade body was determined in the Mechanical APDL thermal calculation.

As a result of the strength calculation, a text file was generated containing information about the static and dynamic strength factors of the rotor wheels:

$\overline{K}_{dl\_m}$ – local long-term strength factor;

$\overline{K}_{dl\_B}$ – long-lasting load-bearing capacity factor;

m_{rb} – mass of a RW working blade;

Δ_{freq1} – reserve as a percentage of the first own blade frequency of RW from the nearest dangerous harmonics;

Δ_{freq2} – reserve as a percentage of the second own blade frequency of RW from the nearest dangerous harmonics.

Values of margins for the frequency detuning Δf_i for the first three natural frequencies of the blades are used as dynamic strength criterion. Margins for the frequency detuning Δf_i are determined as the relative distance between the natural frequency f_i and closest to it harmonics K_i and K_{i+1} (Figure 6):

$$\Delta f_i = \frac{|f_i - K_{i\ closest}|}{|K_{i+1} - K_i|} 100\%$$

where $K_{i\ i\ closest}$ – value of harmonic, closest to i-natural frequency of the blade (K_i and K_{i+1}).

Values of margins for the frequency detuning Δf_i for the first three natural frequencies of the blade must be more than 30% [16].

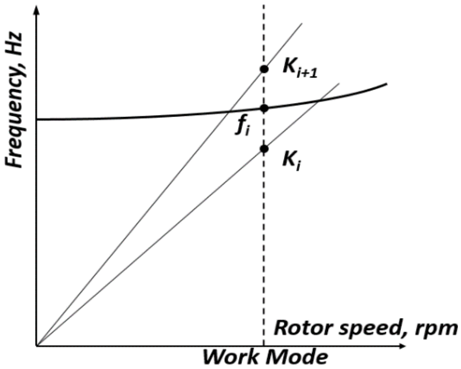

Figure 6 Determination of a parameter Δf_i at Campbell diagram

The calculations determine the maximum stresses in the blade, which were compared with the maximum allowable stresses in the selected material, based on the blade temperature and the required service life.

BLADE SHAPE PARAMETERIZATION SCHEME

A parametric blade model was implemented in the Numeca AutoBlade 5 program. In the optimization process the shape of the blade profiles of the NB and RW was changed, as well as the mutual position of the blade sections at different radii.

The scheme of the parameterization of the profile form used in the research is shown in Figure 7 a. In each variable parametric section, the inlet and exit blade angles, the stagger angle and the chord of the blade were changed. The suction and pressure sides were described by splines, which were parametrically defined by the radius of the inlet and outlet edges, the wedge angle at the outlet, and two points on the pressure side and three points on the suction side.

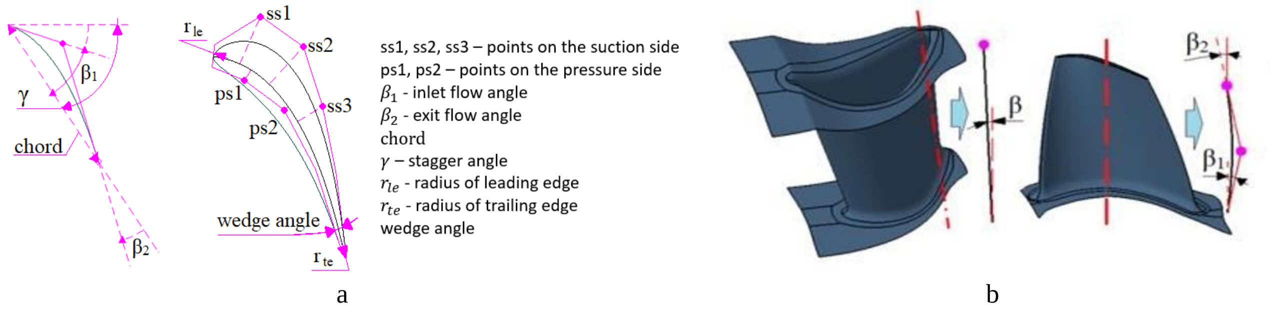

Figure 7 Scheme of turbine blade parameterization

A scheme for parametrization of the mutual position of the blade sections at different radii is shown in 7 b. The position of the section centers of gravity was described by a spline which was defined by an arbitrary number of control points. The used scheme allows to move the sections both in axial and circumferential direction. For the NB of CT, the removal of sections in axial and circumferential directions was defined by 1 variable, and for the RW of CT, by two variables. In the process of solving the optimization task, parametric aerodynamic and strength models operated in a *batch* mode without the use of a graphical interface under the control of a special *.bat* file manager [5].

TURBINE OPTIMIZATION

Initially the CT blades had a strength reserve well below the required values. Therefore, at the initial stage it was decided to engage in the task of strength development of the RW without taking into account aerodynamic processes in order to obtain an initial variant of the blade with a satisfactory strength margin. The obtained variant was used for multidisciplinary optimization of the CT in terms of efficiency and blade weight as a starting point.

The task of optimization was solved step by step. The algorithm for solving the task is shown in Table 2. It shows the char-acteristic features of each solved optimization task, such as whether or not aerodynamic processes are taken into account, the number of varying RW sections, the used blade material, blade temperature distribution and turbine life.

Table 2 Algorithm for finding the required compressor turbine variant

Step		Calculation of aerodynamics	Calculation of the stress state	Blade material	Turbine inlet temperature	Total service life (calculated from long-term endurance)	Number of variable sections of the RW blade	Consideration of technological constraints
1		No	Yes	Initial	Initial	By design	3	No
Result: no solution found								
2		No	Yes	Initial	Initial	By design	5	No
Result: requirements for part of the strength parameters achieved								
3	a	No	Yes	With improved parameters	Reduced by 50K	By design	5	No
	b	No	Yes	With improved parameters	Initial	Reduced by 25%	5	No
	c	No	Yes	With improved parameters	Initial	Reduced by 50%	5	No
4		Yes	Yes	With improved parameters	Initial	By design	5	No
Result: a solution found. Technology is unacceptable For the next step technological constraints are entered								
5	a	Yes	Yes	With improved parameters	Initial	By design	4	Yes
	b	Yes	Yes	With improved parameters	Initial	By design	5	Yes
Result: the decision from step 5a is accepted as final at this step								

Step 1 solved the problem of strength development of the RW without taking into account aerodynamics. At the same time the shape of sections of the working blade according to the scheme of parametrization shown in Figure 7 b in 3 sections (hub, middle and peripheral ones) varied, as well as outgoing sections of RW of CT according to the scheme shown in Figure 7. In addition, the radius of the working blade fillets was changed. The total number of variables in the task was 50.

The criteria for the optimization task were the factors of long-term static and long-term local strength of RW of CT. The restrictions on the optimization task in step 1 were not set.

The solution to step 1 was stopped after about 3,000 calls to the solver by the Optimizer, as there was no further improvement in the criteria. The computational resource consumption per one call to the strength model was about 1 processor-hour. The problem was calculated in parallel on 10 computers.

As a result of the optimization task, the front of Pareto-compromise solutions for local $\bar{K}dlm$ and long-term$\bar{K}dl_B$ strength reserve criteria was formed (Figure 8 a).

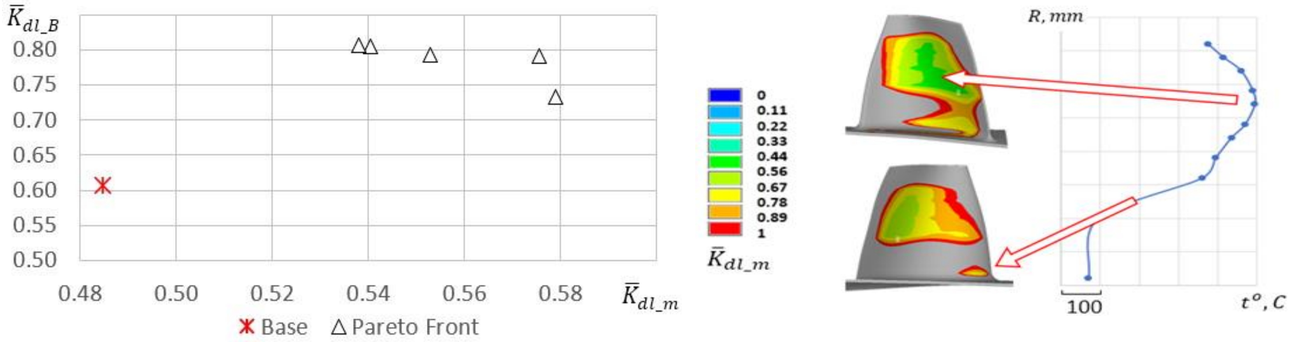

a b

Figure 8 Task of RW finishing of CT step 1: a - Pareto front, b - distribution of local strength reserve depending on the RW temperature

The required value of strength factor was not achieved in the process of solving this problem. The strength factor is caused by two factors: the level of stresses in the blade and the limits on the long-term strength of the material. The limit of the long-term strength of the material is defined by the temperature of the blade material (the given temperature distribution over the blade is shown in the Figure 8 b) and its operating time. The combination of this two factors affecting the local strength factor results in two zones of insufficient strength in the blade of RW. One zone of minimum local strength factor is located in the airfoil blade section about a quarter of the blade height below the peripheral section and is caused by the maximum temperature of the blade at this location. The second zone is located in the blade's fillets and is caused by the maximum stresses from centrifugal force and the high temperature gradient at the point of transition of the root to the airfoil (Figure 8 b).

Analyzing the obtained data, it was concluded that it was not possible to make the strength estimation of the RW using only three parametric sections, as the reduction of the thickness of the peripheral section is accompanied by a reduction of the blade section area by 0.75 relative heights and contributes to the burning of the blade at this location. For this reason, the number of parametric sections in the RW blade was increased to 5 in the next step.

In step 2, a task similar to the step 1 was solved, but the shape of the profiles was changed in five sections. The total number of variables was 78.

Due to the presence of two zones of minimum local long term strength factors, separate long-term local strength factor coefficients for airfoil blade $K_{dl\_m\_blade}$ and for blade fillet $K_{dl\_m\_fillet}$ were entered into consideration.

Local long-term strength factors $K_{dl\_m\_blade}$ in the airfoil and blade fillets $K_{dl\_m\_fillet}$ were adopted as criteria for the optimization task in step 2. Minimum value for long-term static strength margin K_{dl_B} was taken as a restriction. In the process of solving the problem in step 2, about 3.500 optimizer calls were made. The optimization resulted in an increase in the reserve of local long-term airfoil blade strength to the required level, while it was not possible to increase the reserve of local long term strength in the blade fillets.

As a result of the analysis of the obtained data, it was concluded that the limiting factor is the properties of the blade material used by RW. Therefore, it was decided to use a different material with increased strength properties. In addition, in order to ease the search for the initial option, the solution to the task was performed in parallel in three statements with different assumptions. In setting 1, the blade temperature was reduced by 50 degrees, in setting 2 the required turbine resourse was reduced by 25%, and in setting 3 the required turbine life was reduced by 50%.

As a result, in step 3 all three productions were able to find variants of the CT blades that satisfy the strength requirements.

The obtained turbine configuration options were used as the initial step to launch the multi-disciplinary optimization task in step 4, taking into account aerodynamic and strength parameters. At the same time, the configurations were variable:

– variables describing the shape of the hub and peripheral sections of the NB and the five sections of the RW (as shown in Figure 7 a);
– variables describing the axial and circumferential discharge of the NB peripheral section as well as the axial and circumferential discharge of the middle and peripheral sections of RW (as shown in the diagram in Figure 7 a);
– the radius of the working blade fillets;
– the value of static pressure at the outlet of CT (this parameter was a boundary condition of CFD modeling and was necessary to ensure the degree of expansion in the turbine within a given range).

The total number of variables values in the task was 97 variables.

The following restrictions during the optimization were set:

- the value of the working fluid mass flow rate and pressure ratio could not differ by more than 0.5 % from the initial value;
- the reserves of long term static and long term local strength should be no less than the required values.

The optimization criteria were the efficiency of the turbine and the weight of its blade.

In the process of solving the task the intermediate Pareto front was analyzed, which is shown in Figure 9 in parameters of relative weight of the RW blade $\bar{m}_{rb}$ and relative efficiency of the compressor turbine $\bar{\eta}_{CT^*}$ (weight of the RW blade and efficiency of the optimized variants were attributed to the blade weight and efficiency of the initial variant).

To analyze the processability of the working blades after the optimization, the shape of their profiles was compared with the initial CT configuration for the variant with the maximum efficiency. The NB blades changed insignificantly during the optimization process, so the comparison of their profiles is therefore not presented.

From a comparison of the obtained and initial RW profile configurations, it can be seen that the strength restriction was achieved by increasing the profile area in the lower half of the blade. It is interesting to note that the upper quarter of the blade became thicker as well. As a result, an undesirable "wasp-waist" in the profile appeared in the sections at a relative height of 0.75 - a place from which the profile thickness of the blade increases in both directions. In this section, the local thickness was less than the trailing edge thickness and the change in thickness along the profile was non-monotonic. This increased the cost of manufacturing the blade. Therefore, an algorithm was developed that controlled the change in profile thickness (it should increase monotonically from the inlet to the maximum thickness and then decrease monotonically to the trailing edge. It was also controlled that the local profile thickness should be no less than the thickness of the trailing edge.

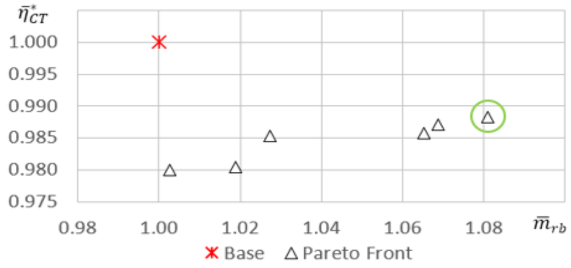

a

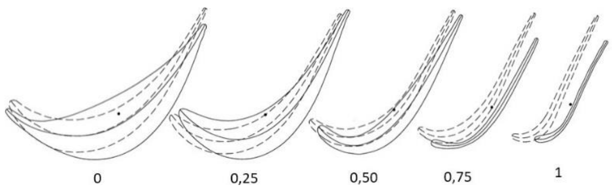

b

FIGURE 9 PARETO FRONT OF STEP 4 OF CT OPTIMIZATION

These circumstances complicate the blade technology. and must be taken into account in the further search for the best turbine configuration. Therefore, a special program was developed to calculate the number of wasp-waists in each blade profile and display this information in the optimization process.

Setting the optimization task at step 5 was identical to setting the task at step 5, but the task was solved in two variants at the same time.

In one task, the form of the RW blades was changed in five sections. In the second task in order to increase processability of the RW CT blade after optimization the shape was changed in four sections due to the fact that the section at the relative height of 0.25 was made dependent on the other sections, i.e. its parameters were calculated from the shape of the other sections according to the cubic spline law [5].

In addition, restrictions on the minimum profile thickness of sections at a relative height of 0.75 and 1, as well as the avoidance of "wasp-waists" in the profile were set. Also in step 5, additional restrictions were set on the minimum thickness of the section profiles at the relative height of 0.75 and 1, and the presence of "wasp-waists" on the profile was monitored. Solving step 5 problems in four and five sections required about 1,000 calls in each formulation at a cost per call of 3 CPU hours. The comparison of two Pareto fronts, obtained as a result of the task solution on step 5 at the change of parameters in the four and five sections of the CT work blades, is shown in Figure 10.

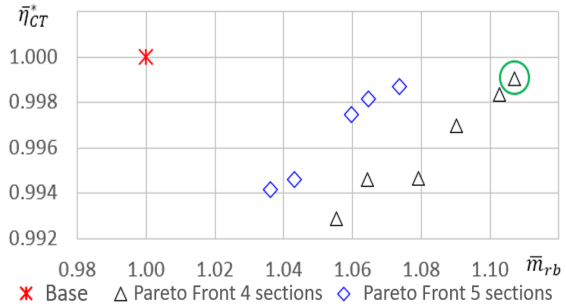

a

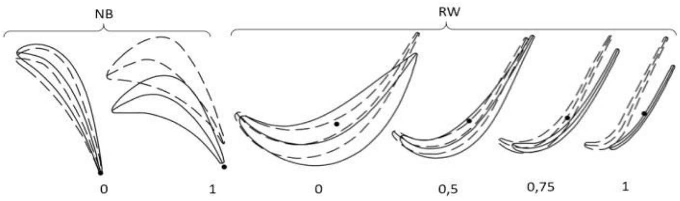

b

FIGURE 10 PARETO FRONT OF STEP 5 OF CT OPTIMIZATION

The check of optimization results on verification model with a grid of finite volumes of high quality showed that the efficiency of optimized CT variant is 0.2 % lower than the initial one at providing the mass flow of the working fluid and the compression degree in the required range.

A comparison of the Mach fields in the original and optimized variants showed a change in the flow structure after the optimization in the CT (Figure 11 a). The factors influencing the efficiency are a more uniform flow structure in the RW CT, reduction of separation currents in the hub section of the RW, but increase of separation currents in the peripheral section of the RW CT.

The strength parameters of the found CT variant are satisfactory. A comparison of the stresses in the CT blade before and after optimization is shown in Figure 11 b. During optimization stresses in the 0.75 relative blade height section were reduced by decreasing the peripheral sectional area of the RW CT. The decrease in stresses in the hub section of the shroud platform was due to an increase in its area. The reduction in stresses in the section below the shroud platform was due to a shift of the labyrinth seal scallop towards the trailing edge. Stresses in the section 0.75 of the relative blade height were reduced by decreasing the peripheral cross-sectional area of the RW CT.

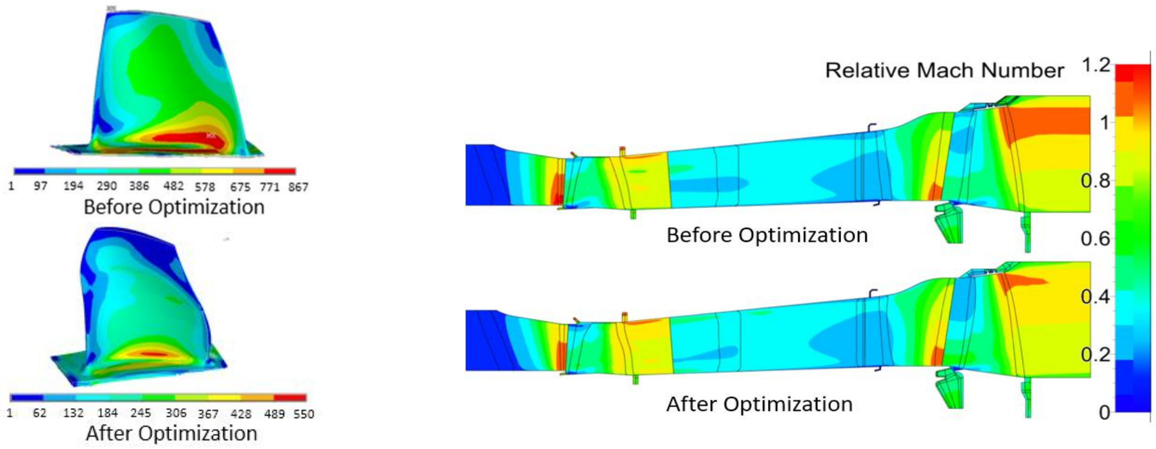

a b

FIGURE 11 COMPARISON OF CT PARAMETERS BEFORE AND AFTER OPTIMIZATION: A - AVERAGE MISES STRESSES IN RW, B - FIELDS OF RELATIVE MACH NUMBER

CONCLUSION

As a result of this work, a complex multi-stage problem aimed at increasing the efficiency of a two-stage axial turbine of a turboshaft engine and ensuring the achievement of the required RW strength margins at meeting technological requirements was solved. The result was achieved by means of multi-stage, multiphysics, multiparametric optimization. A multi-stage cascade of optimization problems was actually solved, during which the area of possible discovery of a variant satisfying multiple and conflicting requirements was gradually refined.

As a result of solving the series of optimization problems, it was possible to eliminate the shortage in the local long-term strength reserve of the RW of CT $\bar{K}dlm$ by 52 % and in the long-term load-bearing capacity reserve of CT $\bar{K}dl\_B$ by 39 % with a drop in efficiency by 0.2 %, which is not significant.

NOMENCLATURE

CT	compressor turbine;
RW	rotor wheel;
NB	nozzle blade;
PS	pressure side
SS	suction side
CFD	computational fluid dynamics;
CPU	central processing unit**;**
$\bar{K}_{d}l_{m}$	relative factor of local long term strength;
$\bar{K}dl\_B$	relative factor of long term bearing capacity;
m_{rb}	mass of a RW working blade;
R	radius;
t	temperature;
$\bar{\eta}CT*$	relative efficiency of the compressor turbine;
$\bar{\eta}^*$	efficiency.

REFERENCES

[1] Iosotech.com. n.d. "Sigma Technology". Novel Optimization Strategy - IOSO. [online] Available at: <http://www.iosotech.com> [Accessed 4 November 2020].

[2] Egorov, I., et al. “IOSO optimization toolkit Novel software to create better design”. *9th AIAA/ISSMO Symposium on*

[3] Matveev, V., et al. “The Optimization of Four-Stage Low Pressure Turbine with Outlet Guide Vane.” *IOP Conference Series: Materials Science and Engineering*. Volume 302, Issue 1, 2018.

[4] Popov, G., et al. “Selection of Parameters for Blade-To-blade Finitevolume Mesh for CFD Simulation of Axial Turbines.” *MATEC Web of Conferences*. Volume 220, 2018.

[5] International, N., n.d. OMNIS™/Turbo & Agile (incl FINE™/Turbo & Agile) | NUMECA International. [online] Numeca.com. Available at: <https://www.numeca.com/product/fineturbo> [Accessed 14 October 2020].

[6] Evgeny Yu. Marchukov E, Yu., Egorov I., Popov G., Salnikov A., Goriachkin E., Kolmakova D. “Multidisciplinary Optimization of the Working Process of Uncooled Axial Turbine According to Efficiency and Strenght Criteria”. *Proceedings of ASME Turbo Expo 2017.* GT2017-64843, 2017